Influence of Particle Size, Precipitates, Particle Cracking, Porosity and Clustering of Particles on Tensile Strength of 6061/SiC$_p$ Metal Matrix Composites and Validation Using FEA

A. Chennakesava Reddy
Professor, Department of Mechanical Engineering
JNTUH College of Engineering Kukatpally,
Hyderabad – 500 085, Telangana, India.
Email: acreddy@jntuh.ac.in

ABSTRACT

Particulate loading, size of particulates, formation of precipitates at the matrix/particle interface, particle cracking, voids/porosity, and clustering of particles may influence the properties of the metal matrix composites. The present research has been focused to anticipate all these effects in 6061/SiCp metal matrix composites. It was found that the tensile strength and stiffness increase with increasing volume fraction of SiC particulates. The tensile strength and stiffness were decreased with increased size of particulates. It was found that the larger particulate crack on account of loading. A clustering of particulates was observed in the composites having very small particles. Formation of Mg_2Si and Fe_3SiAl_2 precipitates were also noticed at the matrix/particle interface. The proposed formulae by the author for the tensile strength and elastic modulus could predict them very close to the experimental values of 6061/SiCp composites.

Keywords - Metal matrix composites (MMCs), strength, analytical modelling, mechanical testing, casting.

1. INTRODUCTION

Metal matrix composite usually consists of a matrix alloy and a discontinuous phase in the form of particulates called the reinforcement. The addition of ceramic particulates into aluminium alloys modify the physical and mechanical properties, assuring high specific elastic modulus, strength-to-weight ratio, fatigue strength, and wear resistance. Silicon carbide particles (SiCp) have demonstrated the most preferred reinforcement materials in metal matrix composites for the automotive and aerospace related applications. Three vital mechanisms manipulate the mechanical properties of such particulate-reinforced metal matrix composites. First, the strengthening mechanism of metal matrix composite based on the load transfer from the metal matrix to the reinforcement imparts higher strength and strain hardening values than those of the matrix material. Secondly, the interface bonding between matrix/particulate is associated with the formation of precipitates. This is strongly dependent on the chemical constituents of the matrix and the wettability of reinforced particulates. Interfacial bonding can be mechanical and chemical. Chemical bonding is significant for particulate metal matrix composites. Thirdly, the deformation behavior is allied with the reinforced particle cracking and particle/matrix delamination upon loading.

The interaction of small size particles with dislocations results in a remarkable improvement of mechanical properties [1]. A chemical reaction at the interface may lead to a strong bond between matrix and reinforcement, but a brittle compound can be highly detrimental to the performance of composite [2]. One of the potential causes for the failure of Al/SiC composites at low tensile strains involves the formation of voids by interfacial debonding [3]. In cast metal-matrix composites, particle clustering is due to the combined effect of reinforcement settling and rejection of the reinforcement particles by the matrix dendrites while these are growing into the remaining liquid during solidification [4]. Particulates must be properly dispersed in order to achieve good wetting and dispersion. This is mostly accomplished by mechanical agitation. The stir casting technology was developed with a two-step stirring for homogeneous particle distribution to prepare particulate metal matrix composites [5, 6]. The precipitation hardening can be improved by heat treatment of the composites [7]. In fact, metal matrix composites have reinforced particles in them, which act to concentrate the stresses locally, effectively causing a localized weakness [8].

When metal matrix composites are manufactured through casting route, there is every possibility of porosity in the composites. When metal matrix composites are made with large size reinforced particulates, at that place is very likely of particle cracking on account of loading. If the composite is prepared with very small particulates, there is a probability of particle clustering. All these phenomena may influence the tensile strength and stiffness of composite. With this underlying background, the motivation for this article is to examine the influence of volume fraction and particle size of SiC$_p$ reinforcement, clustering of particles, the formation of precipitates at the particle / matrix interface, cracking of particles, and voids/porosity on the elastic modulus and tensile strengths of 6061/SiCp metal matrix composites.

2. ANALYTICAL MODELS

For a tensile testing of a rectangular cross-section, the tensile strength is given by:

$$\sigma_t = \frac{F_t}{A_t} \quad (1)$$

The engineering strain is given by:

$$\varepsilon_t = \frac{\Delta L_t}{L_{to}} = \frac{L_t - L_{to}}{L_{to}} \quad (2)$$

where ΔL_t is the change in gauge length, L_0 is the initial gauge length, and L_t is the final length, F_t is the tensile force and A_t is the nominal cross-section of the specimen.

The Weibull cumulative distribution can be transformed so that it appears in the familiar form of a straight line: $Y = mx + b$ as follows:

$$F(x) = 1 - e^{-\left(\frac{x}{\alpha}\right)^{\beta}} \quad (3)$$

$$1 - F(x) = e^{-\left(\frac{x}{\alpha}\right)^{\beta}}$$

$$\ln(1 - F(x)) = -\left(\frac{x}{\alpha}\right)^{\beta}$$

$$\ln\left(\frac{1}{1 - F(x)}\right) = \left(\frac{x}{\alpha}\right)^{\beta}$$

$$\ln\left[\ln\left(\frac{1}{1 - F(x)}\right)\right] = \beta \ln\left(\frac{x}{\alpha}\right)$$

$$\ln\left[\ln\left(\frac{1}{1 - F(x)}\right)\right] = \beta \ln x - \beta \ln \alpha \quad (4)$$

Comparing this equation with the simple equation for a line, we see that the left side of the equation corresponds to *Y*, ln*x* corresponds to *X*, β corresponds to m, and $-\beta\ln\alpha$ corresponds to *b*. Thus, when we perform the linear regression, the estimate of the Weibull parameter (β) comes directly from the slope of the line. The estimate of the parameter (α) must be calculated as follows:

$$\alpha = e^{-\left(\frac{b}{\beta}\right)} \quad (5)$$

According to the Weibull statistical-strength theory for brittle materials, the probability of survival, *P* at a maximum stress (σ) for uniaxial stress field in a homogeneous material governed by a volumetric flaw distribution is given by

$$P(\sigma_f \geq \sigma) = R(\sigma) = e^{-B(\sigma)} \quad (6)$$

Where σ_f is the value of maximum stress of failure, *R* is the reliability, and β is the risk of rupture. A non-uniform stress field (σ) can always be written in terms of the maximum stress as follows:

$$\sigma(x, y, z) = \sigma_{0\,f}(x, y, z) \quad (7)$$

For a two-parameter Weibull model, the risk of rupture is of the form

$$B(s) = A\left(\frac{\sigma}{\sigma_0}\right)^{\beta} \qquad (\sigma_0, \beta > 0) \quad (8)$$

where $A = \int_v [f(x, y, z)]^{\beta} dv \quad (9)$

and σ_0 is the characteristic strength, and β is the shape factor that characterizes the flaw distribution in the material. Both of these parameters are considered to be material properties independent of size. Therefore, the risk to break will be a function of the stress distribution in the test specimen. Equation (8) can also be written as

$$B(\sigma) = \left(\frac{\sigma}{\sigma_A}\right)^{\beta} \quad (10)$$

$$\sigma_A = \sigma[A]^{-\frac{1}{\beta}} \quad (11)$$

And the reliability function, Eq. (11) can be written as a two-parameter Weibull distribution

$$R(\sigma) = e^{-\left(\frac{\sigma}{\sigma_A}\right)^{\beta}} \quad (12)$$

The tensile tests of specimens containing different stress fields can be represented by a two-parameter Weibull distribution with the shape parameter and characteristic strength. The author has proposed expression for the tensile strength considering the effects of reinforced particle size and voids/porosity. The expression of tensile strength is given below:

$$\sigma_t = \sigma_o\left[V_m + V_p - V_v\right]^{-1/\beta} \qquad (\sigma_0, \beta_t > 0) \quad (13)$$

where σ_0 is the characteristic strength of tensile loading, β is the shape parameter which characterize the flaw distribution in the tensile specimen, V_m, V_p, and V_v are respectively volume of the matrix, volume of the reinforced particles and volume of the voids/porosity in the tensile specimen.

3. EXPERIMENTAL PROCEDURE

The matrix alloys and composites were prepared by the stir casting and low-pressure die casting process. The chemical composition of 6061 matrix alloy is given in Table 1. The properties of the matrix alloy and SiCp are given in Table 2. The volume fractions of SiC_p reinforcement are 12%, 16%, and 20%. The particle sizes of SiC_p reinforcement are 10μm, 20 μm, and 30 μm.

Table 1 Chemical composition of alloys

Alloy	Composition determined spectrographically, %								
Element	Al	Si	Fe	Cu	Ti	Mg	Mn	Zn	Cr
6061	97.6	0.62	0.61	0.02	0.053	0.98	0.05	0.07	0.005

Table 2 Mechanical properties of materials

Material	6061 (T6)	SiC
Density	2.7 g/cc	3.21 g/cc
Young's modulus	69 GPa	410 GPa
Ultimate tensile strength	276-310 MPa	310 MPa
Elongation at break	12% (1.6mm thickness)	---
Hardness	95 Brinell (500g load, 10mm ball)	2800 Knoop (Kg/mm^2)
Poisson ratio	0.33	0.14

3.1 Preparation of Melt and Metal Matrix Composites

6061 matrix alloy was melted in a resistance furnace. The crucibles were made of graphite. The melting losses of the alloy constituents were taken into account while preparing the charge. The charge was fluxed with coverall to prevent dressing. The molten alloy was degasified by tetrachlorethane (in solid form). The crucible was taken away from the furnace and treated with sodium modifier. Then the liquid melt was allowed to cool down just below the liquidus temperature to get the melt semi solid state. At this stage, the preheated (500^0C for 1 hour) reinforcement particles were added to the liquid melt. The molten alloy and reinforcement particles are thoroughly stirred manually for 15 minutes. After manual steering, the semi-solid, liquid melt was reheated, to a full liquid state in the resistance furnace followed by an automatic mechanical stirring using a mixer to make the melt homogenous for about 10 minutes at 200 rpm. The temperature of melted metal was measured using a dip type thermocouple. The preheated cast iron die was filled with dross-removed melt by the compressed (3.0 bar) argon gas [5, 6].

3.2 Heat Treatment

Prior to the machining of composite samples, a solution treatment was applied at 500^0 C for 1 hour, followed by quenching in cold water. The samples were then naturally aged at room temperature for 100 hours.

3.3 Tensile Tests

The heat-treated samples were machined to get flat-rectangular specimens (Figure 1) for the tensile tests. The tensile specimens were placed in the grips of a Universal Test Machine (UTM) at a specified grip separation and pulled until failure. The test speed was 2 mm/min (as for ASTM D3039). A strain gauge was used to determine elongation as shown in Figure 2.

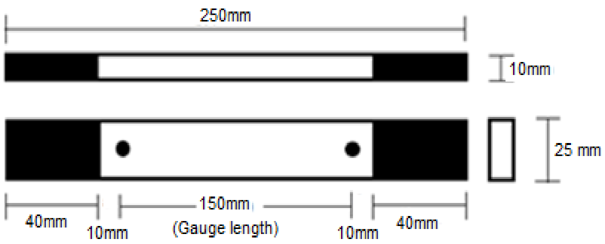

Figure 1 Shape and dimensions of tensile specimen

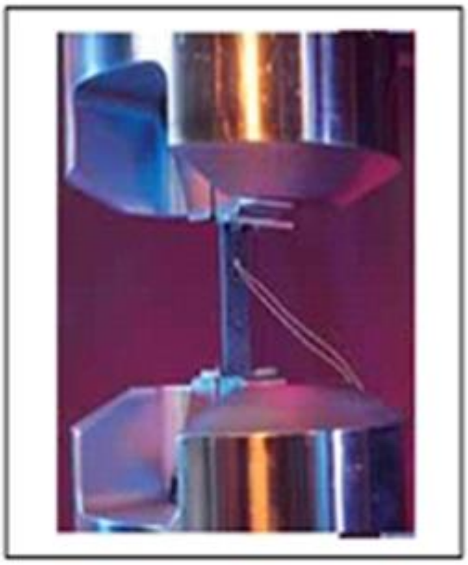

Figure 2 Tensile testing

3.4 Optical and Scanning Electron Microscopic Analysis

An image analyser was used to study the distribution of the reinforcement particles within the 6061 aluminium alloy matrix. The polished specimens were ringed with distilled water, and etched with 0.5% HF solution for optical microscopic analysis. Fracture surfaces of the deformed/fractured test samples were analysed with a scanning electron microscope (SEM) to define the macroscopic fracture mode and to establish the microscopic mechanisms governing fracture. Samples for SEM observation were obtained from the tested specimens by sectioning parallel to the fracture surface and the scanning was carried using S-3000N Toshiba SEM.

3.5 Finite Element Analysis

Particle cracking and porosity in the composite was modelled using ANSYS software. A particle size of 30μm was modelled in a test coupon of 1mm x 1mm composite to examine particle cracking. In addition, a porosity of 100μm was modelled in the test coupon. A triangle element of 6 degrees of freedom was used to mesh the SiC particle and the matrix alloy [9]. For load transfer from the matrix to the particle point-to-point coupling of zero length was used. The test coupon was tensile loaded.

4. RESULTS AND DISCUSSION

The modulus of elasticity is the stiffness of the composite. The modulus of elasticity is improved by the addition of SiC particles because the stiffness of SiC particles is nearly seven times higher that of 6061 aluminium alloy. The metal matrix composites can fail on the microscopic or macroscopic scale. The tensile failure may be either cross-section failure of the workpiece or degradation of the composite at a microscopic scale. The tensile strength is the maximum stress that the material can sustain under a uniaxial loading. For metal matrix composites, the tensile strength depends on the scale of stress transfer from the matrix to the particulates.

4.1 Effect of Particle Size and Volume Fraction on the Tensile Strength

The variation of tensile strength with volume fraction and particle size is shown in Figure 3. It is obviously shown that, for a given particle size the tensile strength increases with an increase in the volume fraction of SiCp. As the particle size increases the tensile strength decreases. This is due to fact that the larger particles have a smaller surface area for transferring stress from the matrix. The strengthening mechanism in the particulate dispersed metal matrix composite is because of obstructing the movement of dislocations and the deformation of material [10]. The amount of obstruction to the dislocations is high for small particles. The other possibility, of increasing strength is owing to the formation of precipitates at the particle/matrix interface. The 6061/SiC derives its strength from Mg_2Si precipitates, which form as needles at the particle/matrix interface. $A1_4C_3$ may be formed by the liquid reaction of 6061 with the SiC particulates. This may not impart precipitation strength to the composite because $A1_4C_3$ is metastable and reacts further to form $MgAl_2O_4$.

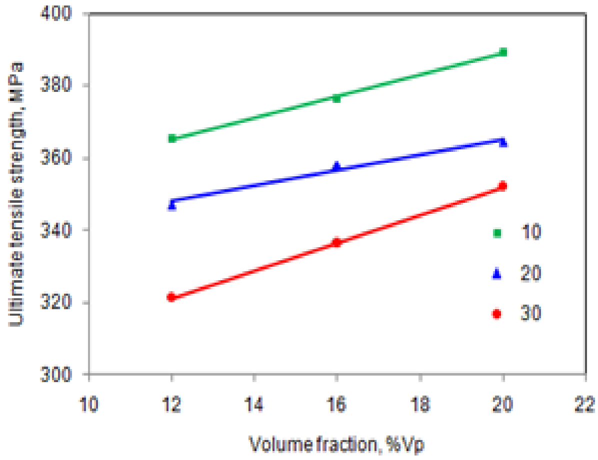

Figure 3 Variation of the tensile strength with the volume fraction and particle size of SiCp

The probability of precipitate formation can be observed in the EDS graph shown in Figure 4. The other strengthening precipitate is Fe_3SiAl_2. This precipitate forms in the composite consisting smaller particulates of SiC as shown in Figure 5. The precipitation hardening also influences the direct strengthening of the composite due to heat treatment. An increase in volume fraction with smaller particles of SiC_p increases the amount of strengthening yet to be paid to increasing obstacles to the dislocations. This is because, smaller particle size means a lower inter-particle spacing so that nucleated voids in the matrix are unable to coalesce as easily.

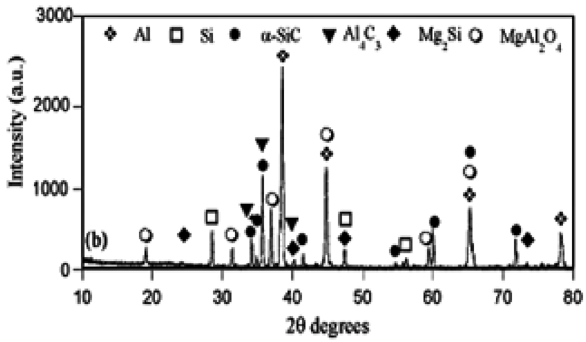

Figure 4 EDS analysis of heat-treated 6061/SiC metal matrix composite (SiC particle size = 20μm and Vp = 20%).

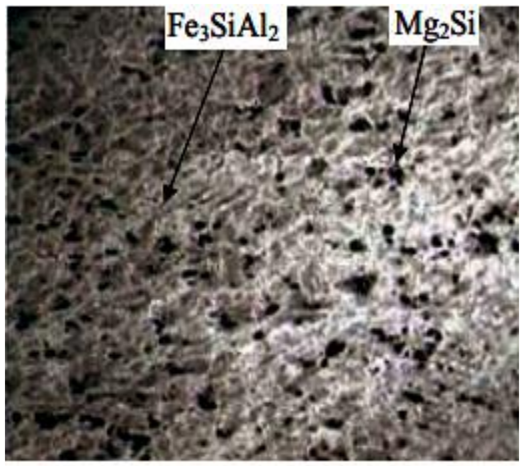

Figure 5 Formation of precipitates in 6061/SiC composite (SiC particle size = 10μm and Vp = 30%).

The coarser particles were more likely to contain flaws, which might severely reduce their strength than smaller particles [11, 12]. Non-planar cracking of particle (Figure 6) was observed in the 6061/SiCp composite comprising 30μm particles. With a single particle of 30μm size in the specimen size of 1mm x 1mm, the particle crack was in the transverse direction of tensile loading. The reduction in tensile strength was about 4.458 MPa. This is because of the low passion's ratio (0.14) of SiC particle as than that (0.33) of the matrix alloy. The SiC particle experiences compressive stress in the transverse direction of tensile loading. There is every possibility of cavity formation during the preparation of composite or during testing of composite due to debonding [13]. The porosity of approximately 100μm was also revealed in the 6061/SiCp composite having 30μm particles as shown in Figure 7. When the porosity of 100μm was incorporated in the specimen size of 1mm x 1mm and analyzed using ANSYS software the strain intensity of 8.427 was observed in the direction of tensile loading.

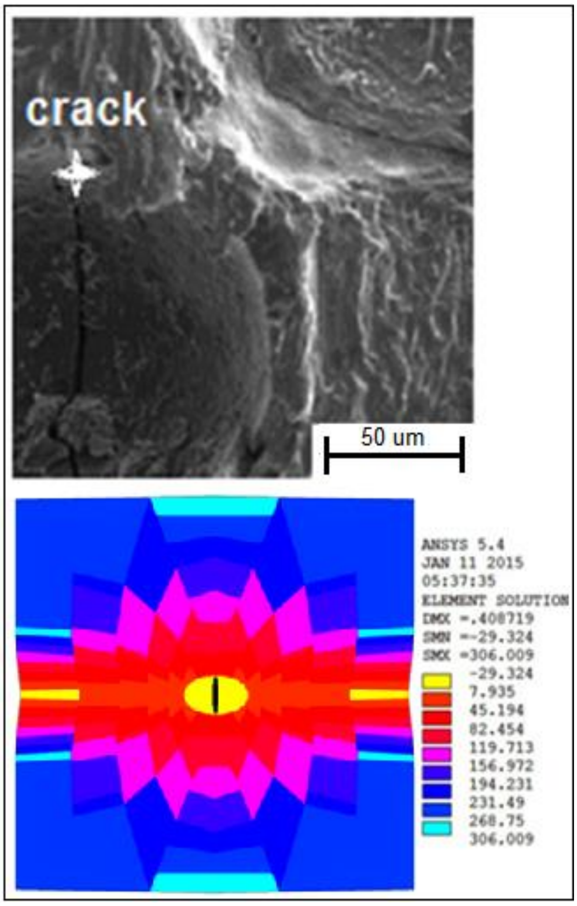

Figure 6 Cracking of SiC particle of 30μm size

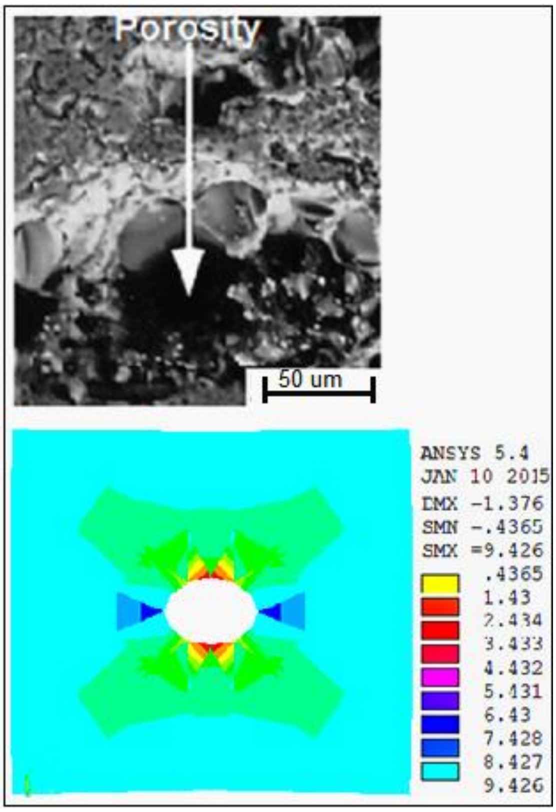

Figure 7 Porosity in 6061/SiC composite (particles of 30μm size and Vp = 20%)

There is a possibility of clustering of SiC particles. These clusters act as sites of stress concentration. At higher volume fractions the particle-particle interaction may develop clustering in the composite. The formation of clustering increases with an increase in the volume fraction and with a decrease in the particle size. Some clusters of smaller particles can be viewed in the untreated filler composite as shown in Figure 8. The number of clusters decreased with decreasing filler loading. The elongation of a tensile specimen decreases with increasing the particle size for given volume fraction as shown in Figure 9.

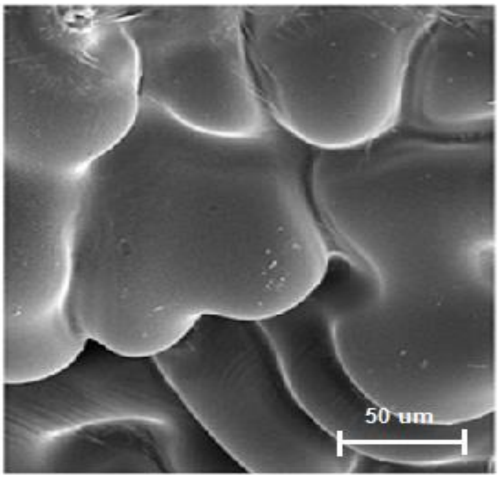

Figure 8 Clustering of SiC particle (10μm) in the composite

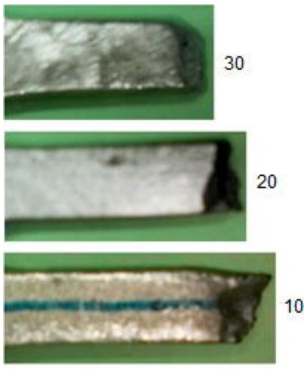

Figure 9 Longitudinal movement (elongation) of material during tensile testing

To sum up, the strength of particulate metal matrix composite can be determined not just by volume fraction, particle size, and particle/matrix interfacial bonding, but also voids/porosity in the composite, particle cracking, formation of precipitates at the particle/matrix interface, an agglomeration of particles, and stress concentration.

4.2 Theories of Strengthening Mechanisms

The strength of a particulate metal matrix composite depends on the strength of the weakest zone and metallurgical phenomena in it. Even if numerous theories of composite strength have been published, none is universally taken over however. Along the path to the new criteria, we attempt to understand them.

Depending on the assumption that the stress cannot be transformed from the matrix to the reinforcement, the strength of a particulate reinforced metal matrix composite was determined from the effective sectional area of load-bearing matrix without reinforcement as given by Danusso and Tieghi [14]:

$$\sigma_c = \sigma_m(1 - v_p) \tag{14}$$

where σ_c and σ_m are, respectively, composite strength and matrix strength, and v_p is particulate volume fraction in the composite. This criterion represents that the composite strength decreases with increasing volume fraction of particulate in the composite as shown in Figure10. This did not include the strengthening mechanism due to the formation of precipitates at the particulate/matrix interface and obstruction to the movement of dislocations and deformation by the particulates. Therefore, this criterion yields the composite strength always lower than that of the matrix.

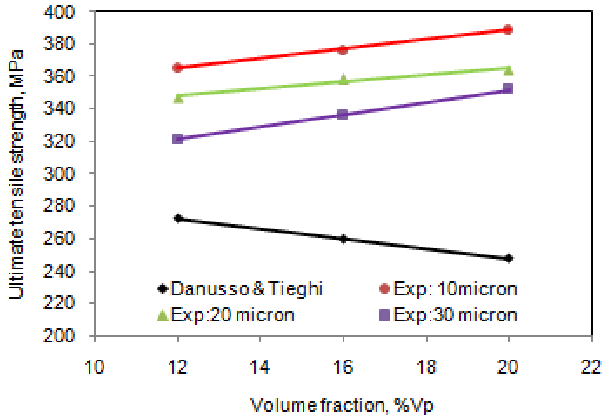

Figure 10 Comparison of Danusso and Tieghi criterion with experimental values

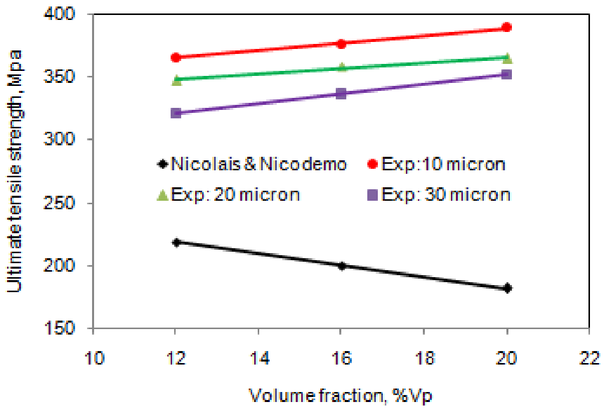

Figure 11 Comparison of Nicolais and Nicodemo criterion with experimental values

Considering adhesion between filler and polymer, a lower-bound strength of the composite was derived by Nicolais and Nicodemo [15]:

$$\sigma_c = \sigma_m\left(1 - 1.21 v_p^{2/3}\right) \tag{15}$$

An upper-bound was obtained by assuming, that the strength of the composite was simply equal to the strength of the matrix. Therefore, the strength is intermediate between these two bounds and cannot be higher than that of the matrix as shown in Figure 11. This measure also did not give any importance to the formation of precipitates at the particulate/matrix interface and obstruction to the movement of dislocations and deformation by the particulates.

Eq. (15) was modified considering the stress concentration of particle volume fraction by Jancar et al. [16]:

$$\sigma_c = \sigma_m\left(1 - 1.21 v_p^{2/3}\right) S_r \tag{16}$$

where S_r is a strength reduction factor and values in the range from 0.2 to 1.0 for high and low volume fractions respectively. When S_r = 1.0, this criterion was equivalent to the criterion proposed by Nicolais and Nicodemo, hence the effect was same.

Eq. (15) was further altered to include some adhesion between matrix and particulates by Lu et al. [17]:

$$\sigma_c = \sigma_m\left(1 - 1.07 v_p^{2/3}\right) \tag{17}$$

As such modification the strength of composites was raised. Yet the issue of particle size and the obstructions of particles of dislocation were not counted. Hence, the predicted strengths of the composites are lower than that of experimentation as shown in Figure12. This standard is fairly more serious than the earlier criteria mentioned above.

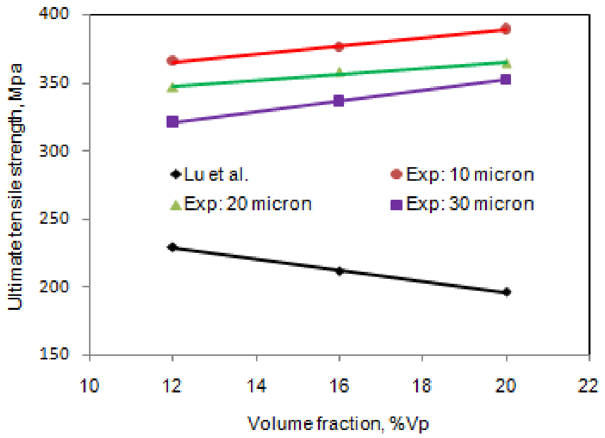

Figure 12 Comparison of Lu et al criterion with experimental values

For very strong particle-matrix interfacial bonding, Pukanszky et al. [18] presented an empirical relationship as given below:

$$\sigma_c = \left[\sigma_m\left(\frac{1 - v_p}{1 + 2.5 v_p}\right)\right] e^{B v_p} \tag{18}$$

where B is an empirical constant, which depends on the surface area of particles, particle density and interfacial bonding energy. The value of B varies between from 3.49 to 3.87. The strength values obtained from this criterion are approaching the experimental values of the composites as shown in Figure13. This criterion has taken care of the presence of particulates in the composite and interfacial bonding between the particle/matrix. The effect of particle size and voids/porosity were not considered in this criterion.

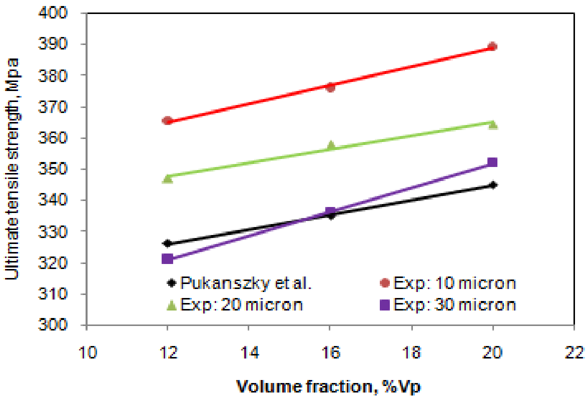

Figure 13 Comparison of Pukanszky et al criterion with experimental values

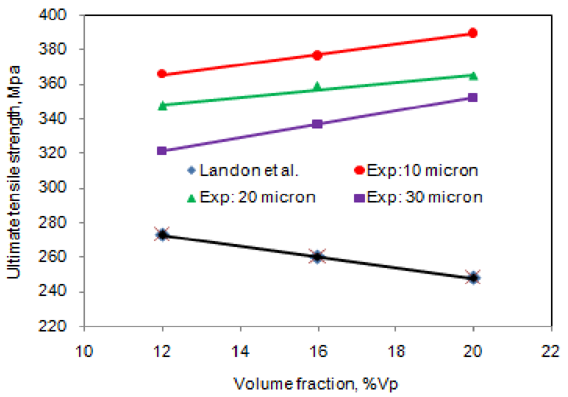

Figure 14 Comparison of Landon et al criterion with experimental values

An empirical linear relationship between composite strength and particle size was projected by Landon et al. [19]:

$$\sigma_c = \sigma_m (1 - v_p) - k(v_p) d_p \qquad (19)$$

where $k(v_p)$ is the gradient of the tensile strength against the mean particle size (diameter) and is a function of particle volume fraction v_p. It can be easily seen that Eq. (19) is an extension of Eq. (18) with an additional negative term on the right side and it predicts a significant reduction in strength by adding particles as shown Figure14. Hence, it is applicable to poorly bonded micro-molecules, but cannot apply to strong interfacial adhesion. It is likewise noted that the variance in the strength is negligible on account of alteration in the particle size.

Hojo et al. [20] found that the strength of silica-filled epoxy decreased with increasing mean particle size d_p according to the relation

$$\sigma_c = \sigma_m + k(v_p) d_p^{-1/2} \qquad (20)$$

where $k(v_p)$ is a constant being a function of the particle loading. This criterion holds good for small particle size, but fails for larger particles as shown in Figure 15. Withal, the composite strength decreases with increasing filler-loading in the composite.

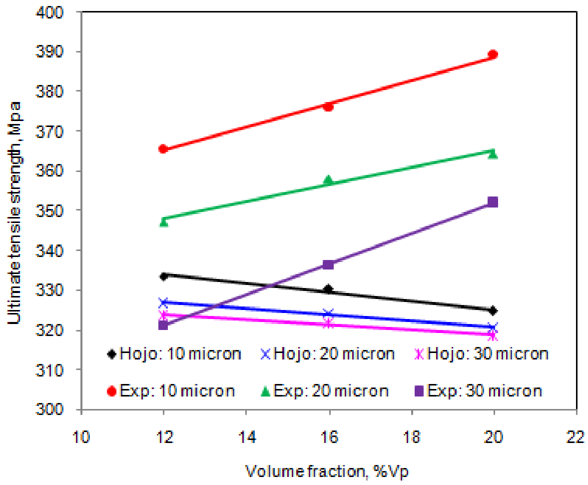

Figure 15 Comparison of Hojo criterion with experimental values

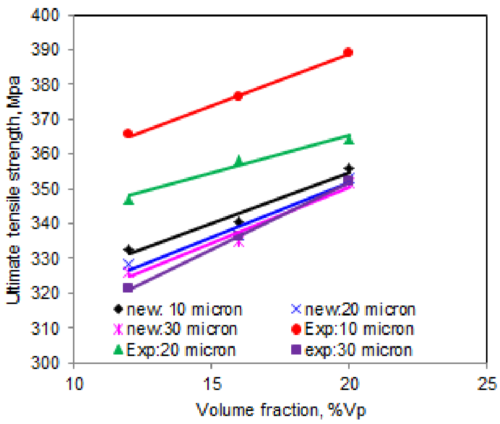

Figure 16 Comparison of proposed criterion with experimental values

A new criterion is suggested by the author considering adhesion, formation of precipitates, particle size, agglomeration, voids/porosity, obstacles to the dislocation, and the interfacial reaction of the particle/matrix. The formula for the strength of composite is stated below:

$$\sigma_c = \left[\sigma_m \left(\frac{1 - (v_p + v_v)^{2/3}}{1 - 2(v_p + v_v)} \right) \right] e^{m_m (v_p + v_v)} + k(v_p) m_p d_p^{-1/2} \qquad (21)$$

where v_v is the volume fraction of voids/porosity in the composite, m_m and m_p are the possion's ratios of the matrix and particulates, and $k(v_p)$ is the slope of the tensile strength against the mean particle size (diameter) and is a function of particle volume fraction v_p. The predicted strength values are within the allowable bounds of experimental strength values as shown in Figure 16.

4.3 Elastic Modulus

Elastic modulus (Young's modulus) is a measure of the stiffness of a material and is a quantity used to characterize materials. Elastic modulus is the same in all orientations for isotropic materials. Anisotropy can be seen in many composites. Silicon carbide (SiC) has much higher Young's modulus (is much stiffer) than 6061 aluminium alloy.

Based on the assumption of rigid particle, Einstein's equation [21] to predict the modulus of elasticity of metal matrix composite is given by:

$$E_c = E_m(1+2.5v_p) \tag{22}$$

where EC and E_m are Young's module of composite and matrix and VP is the volume fraction of particles. Einstein's equation holds good only at low volume fractions of reinforcement and assumes perfect adhesion between particle and matrix, and uniform distribution of reinforced particles. The Young's modulus computed using Einstein's equation is independent of particle size and increases linearly with increasing of particle loading in the composite as mentioned in table 3.

Guth [22] modified the Einstein's equation by adding particle interaction with the matrix as below:

$$E_c = E_m(1+2.5v_p + 14.1v_p{}^2) \tag{23}$$

The second power term in the Guth's equation is an interaction of the strain fields around reinforced particles. Because of the interaction between particles and matrix, the Young's modulus obtained by Guth's equation (Eq.23) is higher than that computed by Einstein's equation (Eq.22).

Kerner [23] found equation for estimating the modulus of a composite that contains spherical particles in a matrix as follows:

$$E_c = E_m\left(1+\frac{v_p}{1-v_p}\frac{15(1-m_m)}{8-10m_m}\right) \tag{24}$$

for $E_p \geq E_m$ and m_m is the matrix poisson's ratio. The modulus of elasticity computed from Kerner's equation is lower than that obtained from Einstein's and Guth's equations as given in table 3.

Mooney [24] prepared another modification to the Einstein equation as follows:

$$E_c = E_m * \exp\left(\frac{2.5v_p}{1-sv_p}\right) \tag{25}$$

where s is a crowding factor for the ratio of the apparent volume occupied by the particle to its own true volume, and its value lies between 1.0 and 2.0.

Counto [25] proposed a simple model for a two phase particulate composite by assuming perfect bonding between particle and matrix. The composite modulus is given by

$$\frac{1}{E_c} = \frac{1-v_p{}^{1/2}}{E_m} + \frac{1}{\left(1-v_p{}^{1/2}\right)/v_p{}^{1/2}E_m + E_p} \tag{26}$$

Ishai and Cohen [26] developed based on a uniform stress applied at the boundary, the Young's modulus is given by

$$\frac{E_c}{E_m} = 1+\frac{1+(\delta-1)v_p{}^{2/3}}{1+(\delta-1)\left(v_p{}^{2/3}-v_p\right)} \tag{27}$$

which is upper-bound equation. They assumed that the particle and matrix are in a state of macroscopically homogeneous and adhesion is perfect at the interface. The lower-bound equation is given by

$$\frac{E_c}{E_m} = 1+\frac{v_p}{\delta/(\delta-1)-v_p{}^{1/3}} \tag{28}$$

where $\delta = E_p / E_m$.

The Young's modulus of particulate composites with the modified rule of mixtures is given by [27]

$$E_c = \chi_p E_p v_p + E_m(1-v_p) \tag{29}$$

Where $0 < \chi_p < 1$ is a particulate strengthening factor.

The proposed equation by the author to find Young's modulus includes the effect of voids/porosity in the composite as given below:

$$\frac{E_c}{E_m} = \left(\frac{1-v_v{}^{2/3}}{1-v_v{}^{2/3}+v_v}\right) + \left(\frac{1+(\delta-1)v_p{}^{2/3}}{1+(\delta-1)\left(v_p{}^{2/3}-v_p\right)}\right) \tag{30}$$

Table 3 Young's modulus obtained from various criteria

Criteria	Young's modulus, GPa		
Criterion	Vp =12	Vp =16	Vp =20
Einstein	89.70	96.60	103.50
Guth	107.91	131.47	161.87
Kerner	83.11	88.71	94.86
Mooney	99.48	116.79	140.95
Counto	105.57	115.009	124.82
Ishai and Cohen (upper bound)	163.43	170.75	178.08
Ishai and Cohen (lower bound)	80.68	85.74	91.35
Rule of mixture (modified)	85.32	90.76	96.2
New proposal from Author	162.30	169.16	176.28

4.4 Weibull Statistical Strength Criterion

The tensile strength of 6061/SiCp was analysed by Weibull statistical strength criterion using Microsoft Excel software. The Weibull shape parameter β indicates whether the failure rate is increasing, constant or decreasing. β <1.0 indicates that the product has a decreasing failure rate. The material is failing during its 'burn-in' period. β =1.0 indicates a constant failure rate. Frequently, components that have survived burn-in will subsequently exhibit a constant failure rate. β>1.0 indicates an increasing failure rate. 6061/SiCp composite indicates increasing failure rate (β values much higher than 1.0). The slope of the line, β, is particularly significant and may provide a clue to the physics of the failure. The Weibull graphs of tensile strength indicate lesser reliability for filler loading of 12% than those reliabilities of 16, and 20 (Figure17). The shape parameters, βs (gradients of graphs) are 18.65, 19.92, and 23.41 respectively, for the composites having the particle volume fraction of 12%, 16%, and 20%.

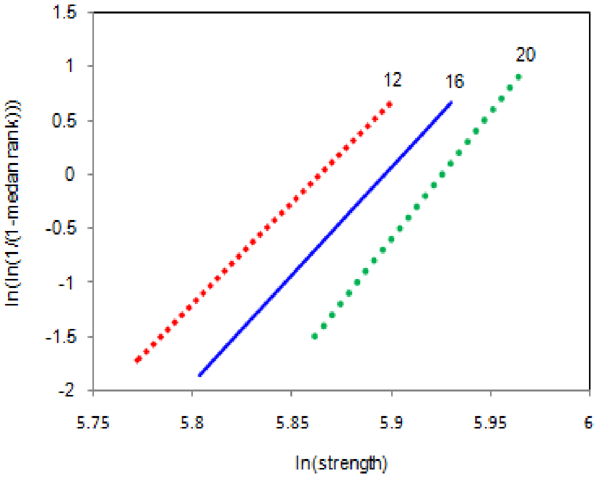

Figure 17 Weibull distribution of tensile strength.

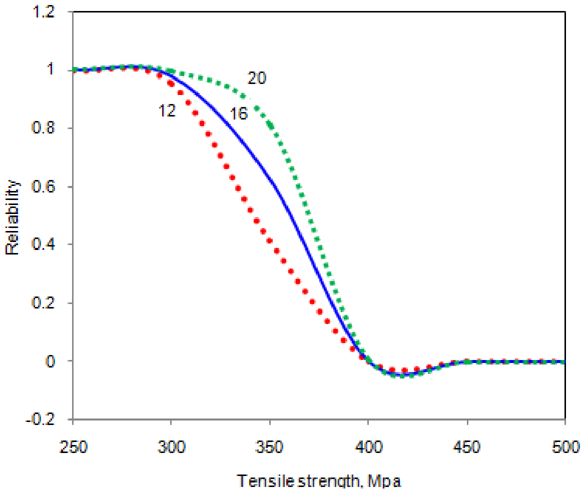

Figure 18 Reliability graphs for tensile strength of /6061/SiCp.

The Weibull characteristic strength is a measure of the scale in the distribution of data. It so happens that 63.2 percent of the composite has failed at σ_0. In other words, for a Weibull distribution R (=0.368), regardless of the value ofβ. With 6061/SiCp, about 36.8 percent of the tensile specimens should survive at least 352.25 MPa, 363.77 MPa, and 374.28 MPa for 12%, 16%, and 20% volume fractions of SiCp in the specimens respectively. The reliability graphs of tensile strength are shown in figure 18. At reliability 0.90 the survival tensile strength of 6061/SiCp containing 12% of volume fraction is 312.21 MPa, 16% of volume fraction is 324.92 MPa, and 20% of volume fraction is 339.98 MPa. This clearly indicates that the tensile strength increases with increase in volume fraction of SiCp.

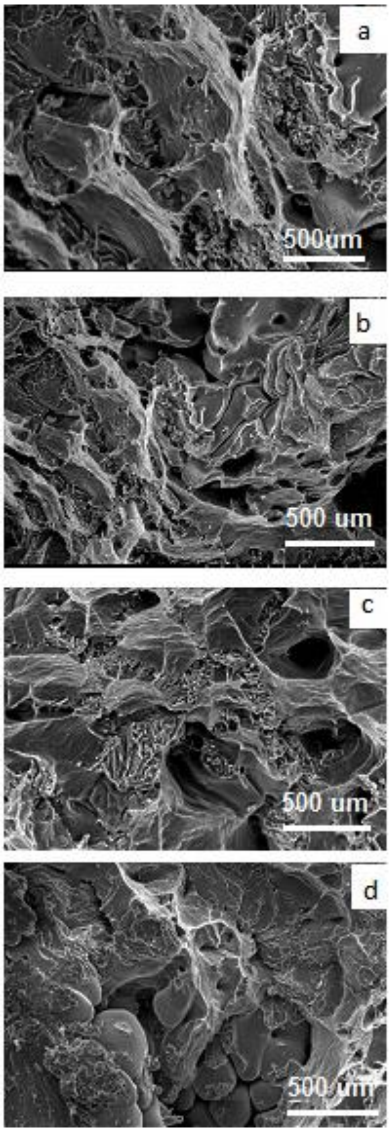

Figure 19 SEM of fracture surface of 6061/SiC composites (a) of 12% Vf and 10 µm particle size of SiC in 6061 (b) of 16% Vf and 10 µm particle size of SiC in 6061 (c) of 16% Vf and 20 µm particle size of SiC in 6061 (d) of 20% Vf and 20 µm particle size of SiC in 6061.

4.5 Fracture

The fracture of SiC particles is not seen in Al 6061/SiC_p metal matrix composites (Figure19). The fracture is only due to the matrix failure and the particle/matrix interface cracking. The fracture process in a high volume fraction (20%) aluminium/SiC_p composite is very much localized. The failure path in these composites is through the matrix due to matrix cracking and the connection of these microcracks to the main crack [28]. Sugimura and Suresh reported that the cracking of SiC particles was a rare event for small size (≤10µm) of particles [29]. There was an incident of particle cracking in case of composite having 30µm size of particulates. The presence of SiC reinforcement particles reduces the average distance in the composite by providing strong barriers to dislocation motion. The interaction of dislocations with other dislocations, precipitates, and SiC particles causes the dislocation motion. The presence of voids is also observed in the composites having larger SiCp particles. The void coalescence occurs when the void elongates to the initial intervoid spacing [30]. This contributes to the dimpled appearance of the fractured surfaces.

5. CONCLUSIONS

The micrographs of 6061/SiCp composites indicate random distribution of SiC_p particles in the metal matrix composites. The EDS report confirms the presence of Mg_2Si and Fe_3SiAl_2 precipitates in the 6061/SiC_p composites. The porosity of approximately 100μm was also revealed in the AA6061/SiCp composite having 30μm particles. At higher volume fractions concentration, i.e., small interparticle distances, the particle-particle interaction may develop agglomeration in the composite. Non-planar cracking of particle was observed in the AA6061/SiCp composite comprising 30μm particles. The tensile strength increases with increase in volume fraction of SiCp, whereas it decreases with increasing particle size. The experimental values of tensile strength and Young's modulus are nearly equal to the predicted values by the new formulae proposed by the authors.

ACKNOWLEDGEMENTS

The author acknowledges with thanks University Grants Commission (UGC) – New Delhi for sectioning R&D project, and Tapasya Casting Private Limited – Hyderabad, and Indian Institute of Chemical Technology – Hyderabad for their technical help.

REFERENCES

[1] Luo, P., McDonald, D.T, Xu. W., Palanisamy, S., Dargusch, M.S., Xia, K. (2012), "A modified Hall–Petch relationship in ultrafine-grained titanium recycled from chips by equal channel angular pressing",Scripta Materialia, Vol. 66, pp 785–788.

[2] Lee, D.J., Vaudin, M.D., Handwerker, C.A., Kattner, U.A. (1988), "Phase Stability and Interface Reactions in the Al-SiC System", Materials Research Society Symposium Proceedings, Proc-120, pp 57-365.

[3] Nutt, S.R., Duva, J.M. (1986). "A failure mechanism in Al-SiC Composites", Scripta Materialia, Vol. 20, pp.1055-1058.

[4] Lloyd, D.J. (1994), "Particle Reinforced Aluminum and Magnesium Matrix Composites", International Material Review, Vol. 39, pp 1-23.

[5] Chennakesava Reddy, A., Essa Z. (2010), "Matrix Al-alloys for silicon carbide particle reinforced metal matrix composites", Indian Journal of Science and Technology, Vol. 3, pp 1184-1187.

[6] Chennakesava Reddy, A., Essa Z. (2009), "Matrix Al-alloys for alumina particle reinforced metal matrix composites", Indian Foundry Journal, Vol.55, pp12-16.

[7] Chennakesava Reddy, A., Kotiveerachari, B. (2010), Effect of aging condition on the structure and properties of Al-alloy/SiC composite", International Journal of Engineering and Technology, Vol.2, pp 462-465.

[8] Chennakesava Reddy, A (2004),"Experimental evaluation of elastic lattice strains in the discontinuously SiC reinforced Al-alloy composites", National Conference on Emerging Trends in Mechanical Engineering, Nagapur, India, VC-12.

[9] Chennakesava R Alavala. (2008), "Finite element methods: Basic concepts and applications", PHI Learning Pvt. Ltd., New Delhi.

[10] Arsenault, R.J. (1988), "Relationship between strengthening mechanisms and fracture toughness of discontinuous SiC/Al composites", Journal of Composites Technology and Research, Vol. 10, Pp 140-145.

[11] Seleznev, M.L., Cornie, J.A., Mason, R.P, Ryal, M.A (1998), "Effect of Composition, Particle Size, and Heat Treatment on the Mechanical Properties of Al-4.5 wt. % Cu based Alumina Particulate Reinforced Composites", In: Proceedings of SAE International Congress and Exposition, Detroit, MI, P. No. 980700.

[12] Lloyd, D.J. (1991), "Aspects of particle fracture in particulate reinforced MMCs", Acta Materialia, Vol. 39, pp 59-72.

[13] Whitehouse, A.F., Clyne, T.W. (1993), "Cavity formation during tensile straining of particulate and short fiber metal matrix composites", Acta Materialia Vol. 41, pp 1701-1711.

[14] Danusso, F., Tieghi, G. (1986), "Strength versus composition of rigid matrix particulate composites", Polymer, Vol. 27, pp 1385-1390.

[15] Nicolasis, L., Nicodemo, L. (1973), "Strength of particulate composite", Polymer Engineering and Science, Vol.13, pp 469-475.

[16] Jancar, J., Dianselmo, A., Dibenedetto, A.T. (1992), "The yield strength of particulate reinforced thermoplastic composites", Polymer Engineering and Science, Vol. 32, pp 1394-1399.

[17] Lu, S., Yan, L., Zhu X., Qi, Z. (1992), Microdamage and interfacial adhesion in glass bead-filled high-density polyethylene, Journal of Material Science, Vol. 27, pp 4633-4638.

[18] Punkanszky, B., Turcsanyi, B., Tudos, F. (1988), "Effect of interfacial interaction on the tensile yield stress of polymer composites", In: H. Ishida, editor, Interfaces in polymer, ceramic and metal matrix composites, Amsterdam: Elsevier, pp 467-77.

[19] Landon, G., Lewis, G., Boden, G. (1977), "The influence of particle size on the tensile strength of

particulate-filled polymers", Journal of Material Science, Vol. 12, pp 1605-1613.

[20] Hojo, H., Toyoshima, W., Tamura, M., Kawamura, N.(1974), "Short- and long- term strength characteristics of particulate-filled cast epoxy resin", Polymer Engineering and Science, Vol. 14, pp 604-609.

[21] Einstein, A. (1905), "Ueber die von der molekular kinetischen fluessigkieten suspendierten teilchen", Annalen der Physik (Leipzig), Vol. 17, pp 549-560.

[22] Guth, E. (1945), "Thoery of filler reinforcement", Journal of Applied Physics, Vol. 16, pp 20-25.

[23] Kerner, E.H. (1956), "The elastic and thermoelastic properties of composite media", Proceedings of Physical Society, Vol. B69, pp 808-813.

[24] Mooney, M. (1951),"The viscosity of a concentrated suspension of spherical particles", Journal of Colloidal Sciience, Vol. 6, pp 162-170.

[25] Counto, U.J. (1964), "Effect of the elastic modulus, creep and creep recovery of concrete", Magazine of Concrete Research, Vol. 16, pp 129-138.

[26] Ishai, O., Cohen I.J. (1967), "Elastic properties of filled and porous epoxy composites", International Journal of Mechanical Sciences, Vol. 9, pp 539-546.

[27] Fu, S.Y., Xu, G., Mai, Y.W. (2002), "On the elastic modulus of hybrid, particle/short fiber/polymer composites", Composite Part B: Engineering, Vol. 33, pp 291-299.

[28] Chennakesava Reddy, A. (2002), "Fracture behaviour of brittle matrix and alumina trihydrate particulate composites", Indian Journal of Engineering & Materials Sciences, Vol. 5, pp 365-368.

[29] Sugimura, Y., Suresh, S. (1992), "Effects of SiC content on fatigue crack growth in aluminium alloy reinforced with SiC particles", Metallurgical Transactions, Vol. 23A, pp: 2231-2342.

[30] Chennakesava Reddy, A., Sundar Rajan, S. (2005) "Influence of ageing, inclusions and voids on ductile fracture mechanism in commercial Al-alloys", Bulletin of Materials Science, Vol. 28, pp 75-79.